A numerical finite element methodology of the EVAR procedure

A. Ramella[1], F. Migliavacca[1], J. F. Rodriguez Matas[1], E. Mariani[2], T. J. Mandigers[3], D. Bissacco[3], A. Freyrie[2], S. Trimarchi [3,4], and G. Luraghi[1]

[1]*Department of Chemistry, Materials and Chemical Engineering "G. Natta", Politecnico di Milano (Italy)*

[2] *Vascular Surgery Unit, Department of Medicine and Surgery, University of Parma (Italy)*

[3]*Department of Clinical and Community Sciences, University of Milan (Italy)*

[4] *Fondazione IRCCS Ca' Granda Ospedale Maggiore Policlinico di Milano (Italy)*

***Abstract* — The abdominal aortic aneurysm (AAA) is one of the most frequent aortic wall pathologies and it is defined as a local dilation of the vessel, typically more than 50% of the physiological diameter. When surgical intervention is needed, AAA can be treated by a minimally invasive technique, endovascular aortic repair (EVAR). EVAR is becoming established as the primary treatment for AAA, given the high short-term success of the procedure. EVAR consists of placing a self-expandable device - called stent-graft (SG) - into the diseased aorta to restore the original lumen. In particular, the device is crimped and placed into a catheter; the catheter is inserted through the femoral artery into the patient and is delivered to the aorta; once the correct position is reached, the catheter is withdrawn, and the SG expands.**

Some studies are present in the literature adopting the finite element analysis to predict the SG behaviour after implantation and its interaction with the aortic wall.

This work aims at recreating stent-graft models similar to commercial ones including both the SGs main body and additional limb extensions and developing a methodology to replicate the EVAR procedure in patient-specific anatomy.

***Keywords* — stent-graft, in silico, FEA, AAA.**

I. INTRODUCTION

THE abdominal aortic aneurysm (AAA) is a localized enlargement of the abdominal aorta such that the diameter is greater than 3 cm or more than 50% larger than nominal. It is a potentially life-threatening condition, as it usually causes no symptoms, except during rupture [1]–[3]. Surgical intervention should be considered when the aneurysm diameter 55 mm, or in the case of rapid growth (>10 mm per year) [2], [4]. In that case, aneurysms can be treated either by open surgery or by an endovascular minimally invasive technique. The minimally invasive technique, called EVAR (endovascular aortic repair), is becoming the primary treatment choice for AAA and consists of placing a self-expandable stent-graft (SG) into the diseased aorta to restore the original lumen [5]. [6]. In particular, the device is crimped and placed into a small delivery system, the catheter. The catheter is then inserted through the femoral artery of the patient, and it is delivered to the aorta; once the correct position is reached, the catheter is withdrawn, and the SG expands [7]. The SG is composed of the stent, a metallic structure, usually made of Nitinol (Nickel-Titanium alloy) or Stainless steel, sutured to the graft, a fabric typically made with either polytetrafluoroethylene (ePTFE) or polyethylene terephthalate (PET)

Despite the high short-term success, the risk of late-onset complications (16-30% of cases [8]) is still present. When a persistent blood flow perfuses the pathological region, endoleaks occur, increasing the risk of rupture of the vessel. Endograft migration is another complication, defined as a SG displacement of 5-10 mm from its original fixation. This could result in endoleaks, and eventually aneurysmal rupture [8].

The Finite Element Analysis (FEA) is largely adopted in the literature to predict the structural behaviour of the SG and the aorta after the EVAR procedure and different approaches are present [9]. In the *virtual shell method* [10], [11] a tubular shell is placed around the device and then morphed to reach the vessel anatomy of the patient. In the *direct placement method* [12], [13] the stent-graft is placed within the patient's aortic lumen through a 3D morphing algorithm. Other studies [14], [15] followed the *virtual catheter method* in which the stent-graft is crimped, deformed by a cylindrical catheter, placed along the vessel centerline and then expanded by removing the catheter. Ramella et al. [16] developed the *tracking method* for the thoracic endovascular aortic repair, in which the stent-graft is crimped into a catheter, displaced along the vessel centerline and then gradually released in the desired aorta landing zone.

In this study CAD models of typical commercial SGs are recreated including both the main bodies and iliac extensions. Then, the *tracking method* is applied to model the EVAR procedure in a patient-specific abdominal aorta replicating both the main body and iliac extension insertion and deployment.

II. MATERIALS AND METHODS

A. Stent-graft CAD models and discretization

For the purpose of the study, two SGs were considered. The SGs are composed of a main body with two leg bifurcations and additional iliac components. The main body in SG1 has a longer ipsilateral leg with respect to SG2. Also, while for SG1 only a straight iliac extension was considered, the SG2 comprised two iliac extensions, a straight and a tapered one. They are suprarenal fixating as the proximal suprarenal stent ring extends above the graft proximally, ensuring the device fixation at the level of the suprarenal arteries.

The CAD modelling procedure to create the SGs main bodies and iliac extensions was performed in SolidWorks (Dassault Systèmes). Considering the stent struts, four types of shapes were identified: Suprarenal, V-type, W-type and

Regular W-type (Fig. 1.a). All the measurements related to the SGs such as diameters, lengths and cross-sections and graft thickness were collected from the literature [17]+(A). Complete models of the two SGs are reported in Fig. 1.b.

The SGs discretization process was performed in ANSA (BETA CAE). The stent rings were discretized using linear two-node beam elements. After a mesh sensitivity, an element size of 0.8 mm was selected. As regards the graft, a free mesh was constructed in ANSA using triangular shell elements with an average length of 0.8 mm and thickness of 0.1 mm (Fig. 2.a). The total number of nodes in the stent and graft for both SG main bodies and iliac extensions is reported in Table I.

The stent and graft in the real device are joined together by some suture points. As they were not directly included in the model, a node-to-node connection between the stent and graft meshes was defined to model the sutures between the two.

Nitinol shape memory material formulation for the stent and a fabric material formulation for the graft were adopted. Details on material parameters can be found in Ramella et al. [16].

TABLE I: NUMBER OF NODES IN THE STENT AND GRAFT FOR EACH STENT-GRAFT COMPONENT

SG component	*#nodes in the STENT*	*#nodes in the GRAFT*
Main body SG1	2464	13297
Main body SG2	2885	10797
Straight iliac extension	1296	7480
Tapered iliac extension	1296	7982

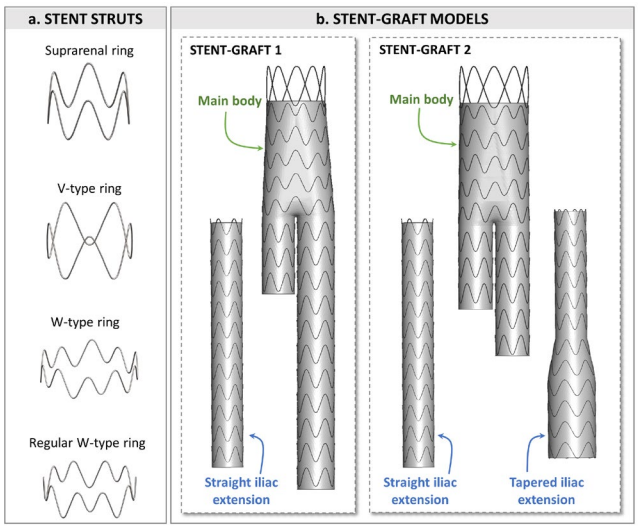

Fig. 1: (a) Different stent struts geometries in the considered stent-grafts; (b) stent-graft 1 (SG1) and stent-graft 2 (SG2) main bodies and limbic extension models recreated for the study.

B. *Aortic model*

Starting from clinical CTA images provided by Azienda Ospedaliera Universitaria di Parma (Italy), a patient-specific model of the aorta was reconstructed through an image segmentation process using the software VMTK (Orobix srl.). The aorta presents an aneurysm in the abdominal region.

The vessel model was discretized using triangular shell elements, with an average target length of 0.8 mm and a thickness of 1.8 mm was assigned [18] (Fig. 2.b). It was modelled as a rigid material as the focus of the methodology is on the SG deployment steps.

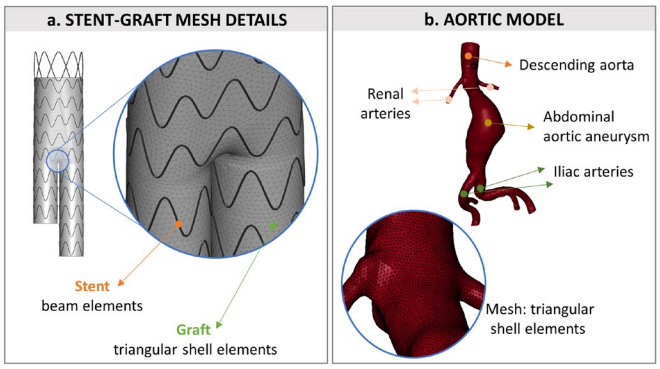

Fig. 2: (a) stent-graft mesh detail; (b) aortic model and mesh detail.

C. *EVAR Finite Element simulation set-up*

During the clinical procedure, the SG is crimped inside a catheter, inserted into the patient through the femoral artery and released into the aorta. As the numerical simulation has to mimic the surgery, these three main steps were simulated starting from the *tracking method* [16] and modifying it for the category of SGs used in the abdominal EVAR procedure.

The EVAR tracking simulation comprises three steps: (1) SG crimping, (2) SG tracking, and (3) SG deployment. In particular, as the SGs included two (SG1) or three parts (SG2), firstly the SG main body was implanted and then the iliac extensions. However, for each component, the simulations follow the three steps listed above.

The two input files (one for SG1 and one for SG2) were created in LsDyna (ANSYS) and included the following parts, as depicted in Fig. 3.a:

- SGs main body and iliac extension meshes;
- SG crimping cylinder was used to perform the device component crimping before the insertion into the femoral arteries.
- Patient-specific rigid aortic model fixed in space.
- Aortic centerlines, which represent the paths for the SGs and extensions displacement in the tracking phase.
- SG catheter, which maintained the SG crimped during the tracking into the aorta. The catheter was modelled as a rigid cylinder morphed on the aortic centerline.

Steps of the simulations for one main body and one iliac extension were reported in Fig. 3.b. In particular, in the first step of the simulation (*crimping phase*), the device was crimped by a cylinder up to a diameter of 10mm. Then, during the *tracking phase*, displacement boundary conditions were imposed on the most proximal stent ring (e.g., suprarenal ring in the case of the SG main body) to displace the device along the vessel centerline within the catheter until the desired landing zone is reached. Lastly, in the *deployment phase*, the SG was gradually released and expanded into the vessel lumen.

During the simulations, soft penalty-based contacts were defined between the SGs and the catheters, between the SGs and the aorta, between the main body legs and between the main body leg and iliac extensions.

For all the simulations, damping was imposed on the stent and graft with a factor equal to 1 ms^{-1} during the crimping, to 0 ms^{-1} during the displacement, and to 5 ms^{-1} during the deployment [16].

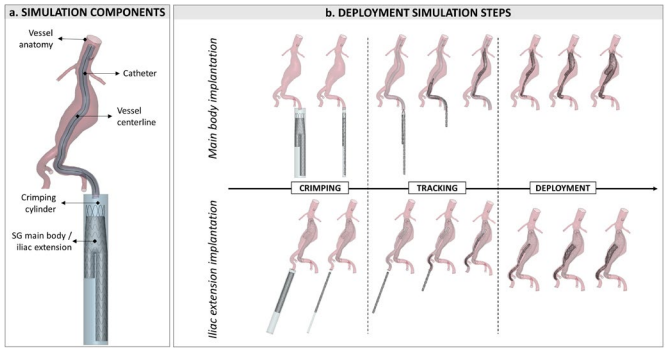

Fig. 3: (a) lists of components involved for the FE simulation; (b) three main steps of the EVAR simulation for the main body and one iliac extension of SG1.

Simulations were run on 20 CPUs with 120 GB of RAM, with a timestep equal to 0.009 ms.

The simulation results were analysed in terms of qualitative deployed configurations, the distance between the SGs and aorta, the maximum principal strain on the graft, and von Mises (VM) stress distribution in the stent and graft.

III. RESULTS

Fig. 4 reports the SGs main bodies and iliac extension deployed configurations.

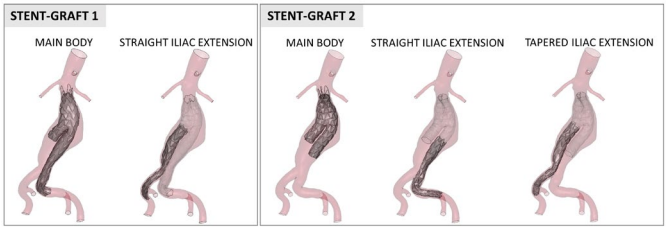

Fig. 4: Main bodies and iliac extensions deployed configurations for the two stent-grafts models

The distance between the device and the vessel is plotted on the aorta (Fig. 5) blue means the SG is completely in contact with the aorta. The distance increases in the aneurysmatic region.

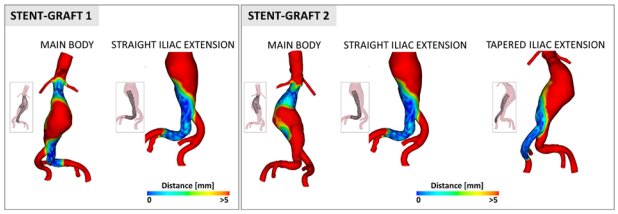

Fig. 5: Distances between the aorta and the main bodies and iliac extensions for both stent-grafts plotted for the vessel.

Maximum Principal Strains are shown in Fig. 6.a. The grafts (both the main body and iliac components) do not fully recover their initial configuration: some folds are present as the vessel has a lower diameter with respect to the initial configuration of the SGs due to the device oversizing. The strains reach higher values in the proximal aortic neck and in the two iliac bifurcations where the vessel is more tortuous and narrower.

Fig. 6.b report the VM Stress distribution on the grafts. The stress is higher in the regions where the grafts are in contact with the vessel, and in the portion of the graft close to the connection with the stent struts. Stresses and strains increase in the main bodies legs after the iliac extension implantation in the overlapped regions (not shown in the figures).

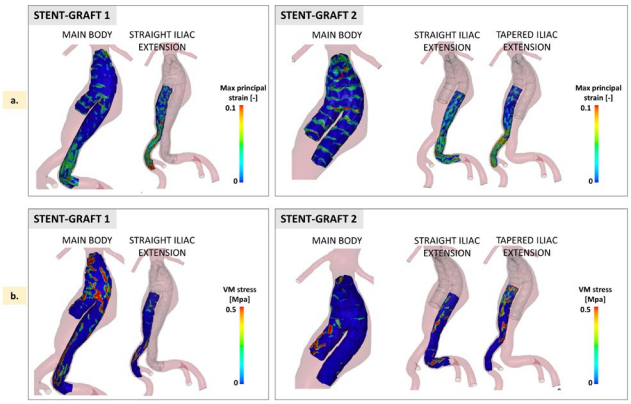

Fig. 6: (a) Maximum principal strain [-] and (b) Von Mises stress [MPa] in the graft of the main bodies (before iliac implantation) and iliac extensions for both stent-grafts.

Fig. 7 reports the VM Stress distribution in the stent struts. In all the configurations, stresses are higher in the regions where the stents are in contact with the vessel (abdominal aortic neck and iliac bifurcations) and in more tortuous regions (e.g., iliac bifurcations). In the aneurysmatic region, stresses are close to zero, as the stent struts have almost completely recovered their original stress-free configuration.

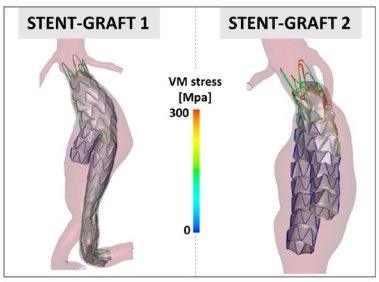

Fig. 7: Von Mises stress distribution in the stent struts for both stent-grafts main bodies.

IV. CONCLUSION

The developed numerical methodology allows simulating the EVAR procedure for the treatment of abdominal aortic pathologies, such as aneurysms. EVAR is a minimally invasive procedure that aims at restoring the physiological fluid dynamics in a pathological vessel by introducing a SG in the interested region [8].

Numerical simulations play an important role in pre-clinical planning to predict the biomechanical interaction between the SG and the aorta [19]. For example, in a pre-procedural patient-specific planning phase, the correct model and size of the device, as well as its positioning into the patient's vessel, can be optimized through FEA.

The present study aims at applying a previously validated methodology – specifically developed for the TEVAR technique – to model the EVAR procedure. Different from other literature methods [9], [11]–[13], the proposed strategy replicate the steps of the real clinical procedure considering also the crimping and gradual release phase for both the main bodies and iliac extensions implantations which could have a major impact on the success of EVAR.

The modelled devices are similar to two commercially available SGs. Both are composed of Nitinol stent rings sutured to a PET graft. To simulate the procedure, finite element domains of the devices were created. A patient-specific aortic model was segmented from clinical CTA images and then discretized. The structural simulation consisted of the following phases: crimping, tracking, deployment of the main body SG into the aorta, and iliac extension implantation. In the first two phases, the main body is crimped and displaced in the correct position of the vessel. During the deployment, the main body is gradually released, entering into contact with the abdominal aorta. During the iliac extension implantation phase, the previous three steps are replicated to implant the additional iliac components within the corresponding main body legs.

This study is not free from limitations. The SGs used in this work were similar to commercial ones but do not include all the peculiarities often found in abdominal SGs as the anchoring hooks, and they were modelled with geometries and materials taken from the literature. More accurate models of commercial SGs can be realized and validated with experimental tests. Also, a rigid aortic model was considered as the focus of the work was on the SGs implantation during EVAR. The EVAR simulation itself might be validated with an ad-hoc experimental set-up as proposed in Ramella et al. [16].

Despite the simplifications, after proper validation, the obtained results can be generalized to any size of a stent-graft and patient-specific deformable anatomies reconstructed from clinical images can be easily adopted for pre-procedural planning, device optimization or, in the future, in-silico clinical trials.

ACKNOWLEDGEMENT

This study has received funding from the MIUR FISR-FISR2019_03221 CECOMES.

REFERENCES

[1] A. Mathur, V. Mohan, D. Ameta, B. Gaurav, and P. Haranahalli, "Aortic aneurysm," *J. Transl. Intern. Med.*, vol. 4, no. 1, p. 35, Apr. 2016, doi: 10.1515/JTIM-2016-0008.

[2] C. Pratesi *et al.*, "Guidelines on the management of abdominal aortic aneurysms: updates from the Italian Society of Vascular and Endovascular Surgery (SICVE)," *J. Cardiovasc. Surg. (Torino).*, vol. 63, no. 3, pp. 328–352, Jun. 2022, doi: 10.23736/S0021-9509.22.12330-X.

[3] A. Wanhainen *et al.*, "Editor's Choice - European Society for Vascular Surgery (ESVS) 2019 Clinical Practice Guidelines on the Management of Abdominal Aorto-iliac Artery Aneurysms," *Eur. J. Vasc. Endovasc. Surg.*, vol. 57, no. 1, pp. 8–93, Jan. 2019, doi: 10.1016/J.EJVS.2018.09.020.

[4] D. K. Owens *et al.*, "Screening for Abdominal Aortic Aneurysm: US Preventive Services Task Force Recommendation Statement," *JAMA*, vol. 322, no. 22, pp. 2211–2218, Dec. 2019, doi: 10.1001/JAMA.2019.18928.

[5] H. O. Kim, N. Y. Yim, J. K. Kim, Y. J. Kang, and B. C. Lee, "Endovascular Aneurysm Repair for Abdominal Aortic Aneurysm: A Comprehensive Review," *Korean J. Radiol.*, vol. 20, no. 8, pp. 1247–1265, Aug. 2019, doi: 10.3348/KJR.2018.0927.

[6] I. C. T. Santos, A. Rodrigues, L. Figueiredo, L. A. Rocha, and J. M. R. S. Tavares, "Mechanical properties of stent-graft materials," *J. Mater. Des. Appl.*, vol. 226, no. 4, pp. 330–341, Oct. 2012, doi: 10.1177/1464420712451065.

[7] "Comparison of endovascular aneurysm repair with open repair in patients with abdominal aortic aneurysm (EVAR trial 1), 30-day operative mortality results: Randomised controlled trial," *Lancet*, vol. 364, no. 9437, pp. 843–848, Sep. 2004, doi: 10.1016/S0140-6736(04)16979-1.

[8] D. D. and T. G. Walker., "Complications of endovascular aneurysm repair of the thoracic and abdominal aorta: evaluation and management. Cardiovascular Diagnosis and Therapy, 8:S138, 4 2018."

[9] S. Avril, M. W. Gee, A. Hemmler, and S. Rugonyi, "Patient-specific computational modeling of endovascular aneurysm repair: State of the art and future directions," *Int. j. numer. method. biomed. eng.*, vol. 37, no. 12, p. e3529, Dec. 2021, doi: 10.1002/CNM.3529.

[10] D. Perrin *et al.*, "Patient-specific simulation of endovascular repair surgery with tortuous aneurysms requiring flexible stent-grafts," *J. Mech. Behav. Biomed. Mater.*, vol. 63, pp. 86–99, Oct. 2016, doi: 10.1016/J.JMBBM.2016.06.013.

[11] D. Perrin *et al.*, "Patient-specific numerical simulation of stent-graft deployment: Validation on three clinical cases," *J. Biomech.*, vol. 48, no. 10, pp. 1868–1875, Jul. 2015, doi: 10.1016/J.JBIOMECH.2015.04.031.

[12] A. Hemmler, B. Lutz, C. Reeps, G. Kalender, and M. W. Gee, "A methodology for in silico endovascular repair of abdominal aortic aneurysms," *Biomech. Model. Mechanobiol.*, vol. 17, no. 4, pp. 1139–1164, Aug. 2018, doi: 10.1007/S10237-018-1020-0/FIGURES/12.

[13] A. Hemmler, B. Lutz, G. Kalender, C. Reeps, and M. W. Gee, "Patient-specific in silico endovascular repair of abdominal aortic aneurysms: application and validation," *Biomech. Model. Mechanobiol.*, vol. 18, no. 4, pp. 983–1004, Aug. 2019, doi: 10.1007/S10237-019-01125-5/TABLES/6.

[14] R. M. Romarowski, E. Faggiano, M. Conti, A. Reali, S. Morganti, and F. Auricchio, "A novel computational framework to predict patient-specific hemodynamics after TEVAR: Integration of structural and fluid-dynamics analysis by image elaboration," *Comput. Fluids*, vol. 179, pp. 806–819, Jan. 2019, doi: 10.1016/J.COMPFLUID.2018.06.002.

[15] X. Kan, T. Ma, J. Lin, W. Lu, and X. Y. Xu, "Patient-specific simulation of stent-graft deployment in type B aortic dissection model development and validation.pdf," *Biomech. Model. Mechanobiol.*, vol. 20, pp. 2247–2258, 2021.

[16] A. Ramella *et al.*, "Validation and Verification of High-Fidelity Simulations of Thoracic Stent-Graft Implantation," *Ann. Biomed. Eng. 2022*, pp. 1–13, Jul. 2022, doi: 10.1007/S10439-022-03014-Y.

[17] X. C. Zhou, F. Yang, X. Y. Gong, M. Zhao, Y. F. Zheng, and Z. L. Sun, "New nitinol endovascular stent-graft system for abdominal aortic aneurysm with finite element analysis and experimental verification," *Rare Met.*, vol. 38, no. 6, pp. 495–502, Jun. 2019, doi: 10.1007/S12598-019-01250-1/FIGURES/10.

[18] M. L. Raghavan, J. Kratzberg, E. M. Castro de Tolosa, M. M. Hanaoka, P. Walker, and E. S. da Silva, "Regional distribution of wall thickness and failure properties of human abdominal aortic aneurysm," *J. Biomech.*, vol. 39, no. 16, pp. 3010–3016, Jan. 2006, doi: 10.1016/J.JBIOMECH.2005.10.021.

[19] G. H. W. van Bogerijen *et al.*, "Contemporary Role of Computational Analysis in Endovascular Treatment for Thoracic Aortic Disease," *Aorta*, vol. 1, no. 3, pp. 171–181, 2013, doi: 10.12945/j.aorta.2013.13-003.